INFLUENCE OF LOCAL BUCKLING ON CYCLIC BEHAVIOR OF STEEL BEAM-COLUMNS

by Isao MITANI[I], Minoru MAKINO[II] and Chiaki MATSUI[III]

SYNOPSIS In order to clarify the influences of local buckling on the hysteretic restoring force characteristics of steel beam-column, cantilever steel columns of H-shape cross section were tested under constant axial load and alternating horizontal load. Three main parameters involved in the tests are the width-to-thickness ratios of the flange and the web and the axial load ratio. Test results clearly show the deterioration of the restoring force due to local buckling, particularly due to the web buckling occuring after the flange buckling. A set of empirical formulas are proposed to relate the plastic deformation capacity of the beam-column to the width-to-thickness ratio of plate elements.

INTRODUCTION Previous research works on the restoring force characteristics of structures have been performed based on the ideal and simplified conditions such that the deterioration of carrying capacity due to lateral buckling of members and local buckling of plates elements does not occur. In actual structures, however, the above mentioned ideal condition is not usually satisfied under the strong earthquake motion, and thus it is important to clarify the effects of lateral and local buckling on the restoring force characteristics of structures, paticularly on the plastic energy absorption capacity of a structure which is the significant measure representing the overall resistance of the structure against strong earthquake disturbances.

A few researches on the influence of local buckling on the behavior of structual steel members were performed. Yamada, et al.[1] and Popov, et al. [2] tested specimens with wide-flange cross section having small width-to-thickness ratios of plate elements, and concluded that the influence of local buckling on the behavior of beams and beam-columns were very small. Fukuchi, et al.[3] obtained empirical relation between rotation capacity and width-to-thickness ratio of the flange, based on the behavior of beams tested under several loading conditions. A similar work was carried out by Adams, et al.[4]. Climenhaga, et al.[5] analysed the post buckling behavior of wide-flange beams, introducing the plastic hinge lines on the plate elements, and showed that the influence of local buckling was considerable. Vann, et al.[6] found that the influences of flange and web local buckling on the hysteretic behavior of wide-flange beam-columns were remarkable.

In most of the works mentioned above, mainly investigated are the correlation between deformation capacity and the width-to-thickness ratio of flange plate elements. Investigated in the present study are the influences of both flange and web local buckling on the cyclic behavior of beam-columns, the experimental results of cantilever steel beam-columns being introduced.

TESTS Figure 1 showed the details of a beam-column specimen, which was tested under constant axial load P and alternating horizontal load H. Loading arrangement is shown in Fig. 2, where the out-of-plane displacement and twisting rotation are prevented at the tip of cantilever specimen. Test

I Lecturer, Faculty of Engineering, Kagoshima Univ., Kagoshima, Japan.
II Professor, Faculty of Engineering, Kyushu Univ., Fukuoka, Japan.
III Associate Professor, Faculty of Engineering, Kyushu Univ., Fukuoka, Japan.

program was composed of two series; fifty six specimens of Series I tested at large amplitude of plastic deflection, i.e., ductility factor μ about 10 to 15, and thirty four specimens of Series II tested at small amplitude, μ=2-5.

Parameters involved in the tests are as follows; b/t, d/w and P/Py, where b is half width of the flange, d depth of the cross section, t and w thicknesses of the flange and the web, and Py the yield axial load. The values of these parameters are tabulated in Table 1, with the name of specimens. The depth and the width of H-shape cross section vary between 100 to 200 mm, and 75 to 135 mm, respectively. Effective slenderness ratio $2\ell/i$ varies between 25 to 40.

H-shape cross sections of specimens, expect for those marked by *, in Table 1, were built up from the mild steel plates of thickness 3.2, 4.5 and 6.0 mm, and high strength steel plate of thickness 6.0 mm. Twelve specimens marked by * were made of rolled H-shape, H-100x100x6x8, their flanges being shaped to have the prescribed ratio of b/t. Six specimens in Series I marked by ** in Table 1 were annealed to leave out the residual stresses, which may affect on the behavior of specimens built up by welding. Test results were compared with those of identical but unannealed specimens marked by ***. Mechanical properties of steel material used are given in Table 2.

HORIZONTAL LOAD-DISPLACEMENT CURVES Several experimental horizontal load (H)-displacement(Δ) curves of Series I and II are shown by solid lines in Figs.3(a) to (c), and 4(a) to (c), respectively. In Fig.3 the results of the initial loading cycle are shown. Marks ▼ and ▽ indicate the points where flange and web local buckling were first observed visually in the tests, respectively. Dashed lines represent the results obtained from the analysis of the deflection of cantilever beam-columns by the numerical integration without consideration of any local buckling. Moment-thrust-curvature relation is calculated for the cross section replaced by a number of small elements, based on the bi-linear hysteretic stress-strain relation of the material, as shown in Fig. 5. Dash-dotted lines represent collapse mechanism lines based on the reduced full plastic moment of the section due to axial load.

From the load-displacement curves obtained in the tests of Series I, the following general observations are induced: In case of specimens having b/t equal to 8, the theory well predicts the experimental behavior until the web buckling occurs, regardless of the values of d/w and P/Py; in case of b/t=11, the decrease in the carrying capacity due to the flange buckling before the web buckling occurs depends on the value of d/w, but is observed to be not very large, regardless of the value of P/Py; the decrease in the carrying capacity of specimens having b/t equal to 16 due to the flange buckling is very severe.

Three distinct types of the hysteretic behavior are clearly observed from the test results of Series II: The first type shown in Fig. 4(a) shows gradually decreasing maximum carrying capacity, which is seen in the following cases: b/t=8 and P/Py=0 regardless of the value of d/w; and b/t=8, d/w< 40, P/Py=0.3 and 0.6. In the second type shown in Fig. 4(b), the decrease in the maximum carrying capacity is quite drastic in each cycle of loading, which is observed in the following cases: b/t=8, d/w>40 and P/Py=0.3; and b/t=11 and 16, P/Py=0.6 regardless of the value of d/w. In the last type shown in Fig. 4(c), the gradual decrease in the maximum carrying capacity is observed after the drastic decrease takes place in the first few cycles, seen in the following cases: b/t=11 and 16, P/Py=0 and 0.3 regardless of the value d/w.

PLASTIC ROTATION CAPACITY Figures 6(a) and (b) show M/M_{pc}-Θ/Θ_{pc} relations obtained from the specimens in Series I at the initial loading cycle. the moment M and rotation Θ are calculated from H and Δ as

$$M=H\cdot\ell+P\cdot\Delta \quad , \quad \Theta=\Delta/\ell \qquad (1a,b)$$

where ℓ denotes the length, and they are non-dimensionalized by the reduced full plastic moment M_{pc} due to axial load and

$$\Theta_{pc}=M_{pc}\cdot\ell/(2\eta\cdot EI) \quad , \quad 2\eta=k^2\cos k/(\sin k-k\cdot\cos k) \qquad (2a,b)$$

where Ei is the flexural rigidity and $k=\ell\cdot\sqrt{P/EI}$. From Fig. 6, it is clearly observed that moment carrying capacity decreases due to flange and web buckling.

Figures 7(a)-(c) show the relations between plastic rotation capacity Rm and ratio $d\sqrt{\sigma_y}/w$, where σ_y is evaluated in ton/cm^2. Rm is defined as

$$Rm=\Theta m/\Theta_{pc}-1 \qquad (3)$$

where Θm is the rotation corresponding to the point where the maximum moment Mmax is attained. If $M_{max}<M_{pc}$, Rm is taken equal to 0. Dashed lines given by

$$Rm=9.9-0.0157\ (d\sqrt{\sigma_y}/w) \quad \text{for } P/Py=0 \qquad (4a)$$

$$Rm=10.8-0.100\ (d\sqrt{\sigma_y}/w) \quad \text{for } P/Py=0.3 \qquad (4b)$$

are empirical formulas deduced by the least squares from experimental results of specimens having the value of $b\sqrt{\sigma_y}/t$ about 15. For P/Py=0.6, the formula could not be obtained because of few experimental data.

Guide to the Plastic Design of Steel Structures[7] recently published by Architectural Institute of Japan indicates the limiting value of $b\sqrt{\sigma_y}/t$ to be 15. Dash-dotted lines in Fig. 7 indicate the limiting value of $d\sqrt{\sigma_y}/w$ suggested by the Guide. Substituting the limiting values of $d\sqrt{\sigma_y}/w$ suggested by the Guide into Eqs.(4a,b) leads to the values of Rm equal to about 8 and 4, corresponding to P/Py=0 and 0.3, respectively. In Fig. 7 the data for $b\sqrt{\sigma_y}/t$ =20 and P/Py=0 indicate that the value of Rm depends on the value of $d\sqrt{\sigma_y}/w$, but always exceeds 1 in the region where the value of $d\sqrt{\sigma_y}/w$ is less than the limiting value by the guide. The data for $b\sqrt{\sigma_y}/t$=27-30 and P/Py=0, and for $b\sqrt{\sigma_y}/t$ 20 and P/Py=0.3 indicate that the value of Rm is constantly equal to about 1.

PLASTIC ENERGY ABSORPTION CAPACITY Figures 8(a)-(c) show the relations between non-dimensional accumulated energy absorbed by the specimen $\sum e$ and non-dimensional accumulated plastic displacement $\sum\delta p$. $\sum e$ and $\sum\delta p$ are defined as follows:

$$\sum e=(\sum\Delta W)/(Hpc\cdot\Delta pc) \quad , \quad \sum\delta p=(\sum\Delta p)/\Delta pc \qquad (5a.b)$$

Suppose that a H-Δ hysteretic loop is drawn at a certain loading stage, as shown in Fig.8(b), quantities appearing in Eq.(5) are defined as follows: ΔW denotes the area of the loop, Δp plastic displacement involved in the loop, Hpc and Δpc the load and displacement at the intersection of the rigid-plastic mechanism line and elastic line. When to evaluate $\sum e$ and $\sum\delta p$ by Eq.(5), loops in which the maximum load carrying capacity in below the mechanism line are not included. It is observed from Fig. 8 that the value of $\sum e$ is considerably reduced by the increase in the value of width-to-thickness ratios of the flange and the web. However it is interesting to note that approximately linear relations are observed between $\sum e$ and $\sum\delta p$, independently of the values of b/t and d/w, in each Fig. 8(a)-(c). Therefore, the plastic energy absorption capacity may be evaluated in terms of cyclic deformation capacity $\sum\delta p$.

The values of $\sum\delta p$ are plotted against arguments of $d\sqrt{\sigma y}/w$ in Figs. 9(a) -(c), where dashed line expresses an empirical formula

$$\log(\sum\delta p)=2.42-0.0112\cdot d\sqrt{\sigma y}/w \quad \text{for } P/Py=0.3 \qquad (6)$$

obtained from the data for $b\sqrt{\sigma y}/t$=15. Similar approximation could not be done

for P/Py=0 and 0.6, because of few experimental data, but however it should be noted that the value of $\sum\delta p$ given by Eq.(6) is conservative for the cases P/Py=0 and 0.6, since if the value of $d\sqrt{\sigma y}/w$ is identical, the value of $\sum\delta p$ for P/Py=0.3 is less than those for P/Py=0 and 0.6, as observed in Fig. 8. As observed in Fig. 9, the data for $b\sqrt{\sigma y}/t>20$ show the clear influence of $d\sqrt{\sigma y}/w$ on the cyclic plastic deformation capacity, which differs from the tendency observed in Rm-$d\sqrt{\sigma y}/w$ relations in Fig. 7. For specimens having the value of $b\sqrt{\sigma y}/t$ larger than 20, the cyclic plastic deformation capacity may be hardly expected in the region where $d\sqrt{\sigma y}/w>70$, regardless of the value of P/Py.

INFLUENCE OF RESIDUAL STRESSES Typical patterns of residual stress distribution obtained from built-up specimens are shown in Fig. 10. The residual stress pattern in the cross section near the bottom of the specimen differs from that near the center because of the welding to fix the specimen to the base. M/Mpc-θ/θpc relations of unannealed and annealed specimens shown in Fig. 11 by solid and dotted lines, respectively, in which the influence of the residual stress is clearly observed.

SUMMARY AND CONCLUSION The behavior of steel beam-columns under constant axial load and alternating horizontal load is experimentally investigated using H-shape column specimens with various values of the width-to thickness ratios of the flange and the web and the axial load ratio. Test results show that the influence of the local buckling on the restoring force characteristics is quite large. The drastic deterioration of the carrying capacity is observed in the tests due to the web buckling which occurs after the flange buckling, although the value of the specimen satisfies the requirement for the plastic design. In view of the test results, the plastic deformation capacity and plastic energy absorption capacity are empirically estimated in terms of the width-to-thickness ratio.

REFERENCES

1. M. Yamada and T. Takagi : ELASTIC-PLASTIC BEHAVIOR OF WIDE-FRANGE STEEL BEAM-COLUMN SUBJECTED TO HORIZONTAL FORCE AND CONSTANT AXIAL LOAD(About Influence of Local Buckling of Plate Element on Load Carrying Capacity), Proc. Annual Meeting of Architec. Inst. of Japan, Oct. 1968, pp.991-992 (in Japanese).
2. E.D.Popov and R.B.Pinkney : RELIABILITY OF STEEL BEAM-TO-COLUMN CONNECTIONS UNDER CYCLIC LOADING, Proc. 4th WCEE, 1969, Santiago-Chile, B-3, pp.15-30.
3. Y. Fukuchi and M. Ogura : EXPEIMENTAL STUDIES ON LOCAL BUCKLING AND HYSTERETIC CHARACTERISTICS ON H-SHAPE BEAMS, Trans. Architec. Inst. of Japan, No.228, Feb. 1975, pp.65-71 (in Japanese).
4. A.F.Lukey and P.F.Adams : ROTATION CAPACITY OF BEAMS UNDER MOMENT GRADIENT, Proc. ASCE, Vol.95, No.ST6, June 1969, pp.1173-1188.
5. J.J.Climenhaga and R.P.Johnson : MOMENT-ROTATION CURVES FOR LOCALLY BUCKLING BEAMS, Proc. ASCE, Vol.98, No.ST6, June 1972, pp.1239-1254.
6. W.P.Vann, L.E.Thompson, L.E.Whally and L.D.Ozier : CYCLIC BEHAVIOR OF ROLLED STEEL MEMBERS, Proc. 5th WCEE, Vol.1, Rome, 1973.
7. Architectural Institute of Japan : Guide of the Plastic Design of Steel Structures, 1975.

Table 1 Test Program

NAME	b/t	d/w	P/Py	$2\ell/i$	member	flange	web	
I-060A	6.2	16.5	0	35.1	H-100x100	R1	R2	*
I-063A	6.2	16.5	.30	35.2	x6x8	"	"	*
I-066A	6.3	16.5	.60	35.1		"	"	*
I-080A	8.6	17.1	0	35.9	H-100x100	A5	A5	
I-083A	8.7	17.2	.28	35.7	x6x6	"	"	
I-086A	8.6	17.0	.59	35.6		"	"	
I-080B	7.9	22.1	0	35.2	H-100x100	A1	B1	
I-083B	8.2	22.2	.28	35.0	x4.5x6	"	"	
I-086B	8.0	22.2	.55	35.0		"	"	
I-080C	8.1	30.4	0	34.4	H-100x100	A1	C1	
I-083C	7.9	30.6	.28	34.1	x3.2x6	"	"	
I-086C	8.0	30.5	.60	34.4		"	"	
I-080D	7.5	43.1	0	33.8	H-135x100	A3	C3	
I-083D	7.6	43.2	.30	33.8	x3.2x6	"	"	
I-080E	8.1	54.4	0	27.1	H-170x100	A3	C3	
I-083E	8.3	54.0	.30	27.3	x3.2x6	"	"	
I-090A	9.0	15.7	0	37.2	H-100x100	R1	R2	*
I-093A	8.8	15.7	.30	37.2	x6x5.5	"	"	*
I-096A	8.6	15.8	.0	36.9		"	"	*
I-110A	11.5	15.3	0	38.5	H-100x100	R1	R2	*
I-113A	11.5	15.3	.30	38.5	x6x4.4	"	"	*
I-116A	11.8	15.3	.60	38.6		"	"	*
I-110B	11.1	22.2	0	35.3	H-100x100	B1	B1	
I-113B	11.1	22.4	.25	35.4	x4.5x4.5	"	"	
I-116B	11.1	22.3	.49	35.3		"	"	
I-110C	11.1	30.9	0	34.7	H-100x100	B1	C1	
I-113C	11.1	30.9	.25	34.5	x3.2x4.5	"	"	
I-116C	11.1	30.6	.51	34.1		"	"	
I-110E	10.9	55.1	0	27.4	H-170x100	B3	C3	
I-113E	11.0	54.4	.30	27.7	x3.2x4.5			
I-160A	15.9	15.0	0	40.2	H-100x100	R1	R2	*
I-163A	16.0	14.9	.30	40.3	x6x3.2	"	"	*
I-166A	15.1	15.0	.60	40.0		"	"	*
I-160C	15.3	30.4	0	34.8	H-100x100	C1	C1	
I-163C	15.4	30.7	.26	34.9	x3.2x3.2	"	"	
I-166C	15.3	30.6	.52	35.1		"	"	
I-160D	15.6	42.8	0	34.9	H-135x100	C3	C3	
I-163D	15.7	42.4	.30	35.3	x3.2x3.2	"	"	
I-160E	15.7	53.6	0	28.6	H-170x100	C3	C3	
I-163E	15.7	53.6	.30	28.6	x3.2x3.2	"	"	
I-160F	15.9	63.7	0	24.7	H-200x100	C3	C3	
I-163F	15.9	63.7	.30	24.7	x3.2x3.2	"	"	
I-H-060B	6.0	21.6	0	37.0	H-135x75	HT	HT	
I-H-063B	6.2	22.3	.30	36.6	x6x6	"	"	
I-H-066B	6.2	22.3	.60	36.6		"	"	
I-H-110B	10.6	21.6	0	34.4	H-135x135	HT	HT	
I-H-113B	10.6	21.6	.30	34.4	x6x6	"	"	
I-H-116B	10.6	21.2	.60	34.6		"	"	
I-080Cw	8.6	30.3	0	34.7	H-100x100	A4	C4	***
I-083Cw	8.6	32.4	.30	34.6	x3.2x6	"	"	***
I-160Cw	15.0	30.3	0	34.7	H-100x100	C4	C4	***
I-163Cw	15.1	31.6	.30	34.4	x3.2x3.2	"	"	***
I-080Ca	8.6	29.9	0	34.7	H-100x100	AA	CA	**
I-083Ca	8.6	30.7	.30	34.3	x3.2x6	"	"	**
I-160Ca	15.2	29.9	0	35.2	H-100x100	CA	CA	**
I-163Ca	14.7	31.4	.30	34.4	x3.2x3.2	"	"	**

NAME	b/t	d/w	P/Py	$2\ell/i$	Δ_a/Δ_{pc}	member	flange	web
II-080A	8.7	17.1	0	34.9	±5.0	H-100x100	A5	A5
II-083A	8.7	17.1	.30	35.9	"	x6x6	"	"
II-086A	8.7	17.1	.60	35.7	"		"	"
II-080B	8.3	22.4	0	35.1	±5.0	H-100x100	A2	B2
II-083B	8.2	22.6	.30	34.7	+5.1	x4.5x6	"	"
II-083B'	7.9	22.1	.30	34.7	+5.0		A1	B1
II-086B	8.3	22.6	.60	34.7	+5.1		A2	B2
II-080C	8.1	30.6	0	34.1	±5.0	H-100x100	A2	C2
II-083C	8.1	30.6	.30	34.3	"	x3.2x6	"	"
II-086C	8.0	30.4	.60	34.2	"		"	"
II-080D	7.6	43.5	0	33.6	±4.8	H-135x100	A3	C3
II-083D	7.6	43.3	.30	33.7	±5.0	x3.2x6	"	"
II-083E	7.4	54.5	.30	27.1	±4.9	H-170x100 x3.2x6	A3	C3
II-110B	11.2	22.3	0	35.3	±5.0	H-100x100	B1	B1
II-113B	11.1	22.2	.30	35.3	±3.0	x4.5x4.5	"	"
II-116B	11.1	22.3	.60	35.1	±3.0		"	"
II-110C	11.1	30.9	0	34.3	±5.0	H-100x100	B1	C1
II-113C	11.1	30.6	.30	34.5	±3.0	x3.2x4.5	"	"
II-116C	11.1	30.4	.60	34.4	±3.0		"	"
II-113E	11.0	54.4	.30	27.8	±2.0	H-170x100 x3.2x4.5	B3	C3
II-160C	16.1	31.8	0	35.1	±1.7	H-100x100	C2	C2
II-160C'	15.3	30.9	0	34.8	±5.0	x3.2x3.2	C1	C1
II-163C	16.1	32.3	.30	35.0	±1.8		C2	C2
II-166C	16.2	31.7	.60	35.1	±1.4		"	"
II-163D	15.6	43.0	.30	34.8	±2.0	H-135x100 x3.2x3.2	C3	C3
II-163E	15.7	53.9	.30	28.5	±2.0	H-170x100 x3.2x3.2	C3	C3
II-160F	15.8	63.4	0	24.6	±1.9	H-200x100	C3	C3
II-163F	15.6	64.0	.30	24.8	±1.5	x3.2x3.2	"	"
II-H-060B	6.0	21.6	0	36.6	±3.0	H-135x75	HT	HT
II-H-063B	5.9	21.3	.30	36.6	±3.0	x6x6	"	"
II-H-066B	5.9	21.4	.60	36.8	±3.0		"	"
II-H-110B	10.6	21.6	0	34.2	±3.0	H-135x135	HT	HT
II-H-113B	10.7	21.4	.30	34.6	±3.0	x6x6	"	"
II-H-116B	10.7	21.4	.60	34.6	±3.0		"	"

2b: width of flange, t: thickness of flange, d: depth of the cross section, w: thickness of web, ℓ: specimen length, i: radius of gyration about strong axis of the cross section, Δ_a: deflection amplitude, Δ_{pc}: plastic deflection at first hinge formed (2nd order elastic-plastic analysis), flange and web: corresponding to plate name in Table 2.

Table 2 Mechanical Properties

PLATE	σ_y (t/cm²)	σ_u (t/cm²)	ε_{st} (%)	ε_b (%)
A1	3.00	4.57	2.23	33.6
A2	3.06	4.36	2.15	31.3
A3	3.18	4.47	2.08	27.9
A4	3.26	4.74	2.18	27.3
A5	3.12	4.57	2.35	32.9
B1	3.31	4.82	1.99	29.8
B2	2.99	4.61	1.50	29.8
B3	3.38	4.43	1.15	24.2
C1	3.22	4.51	1.15	27.3
C2	3.52	4.62	1.99	26.9
C3	2.94	3.75	1.98	26.1
C4	2.77	3.44	2.38	28.8
R1	3.03	4.68	1.88	24.8
R2	3.31	4.75	2.08	24.7
HT	4.65	5.49	3.83	25.4
AA	2.99	4.48	2.29	29.0
CA	2.39	3.24	3.50	32.9

σ_y; yield point stress
σ_u; tensile strength
ε_{st}; strian-hardening strain
ε_b; maximum elongation

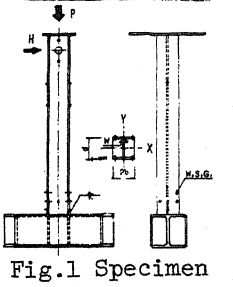

Fig.1 Specimen

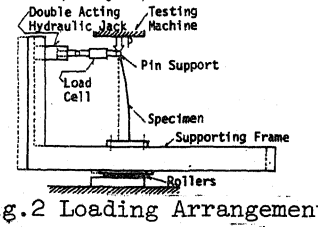

Fig.2 Loading Arrangement

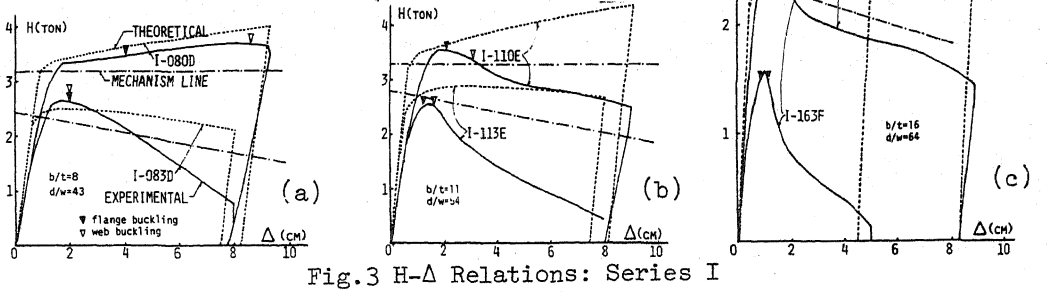

Fig.3 H-Δ Relations: Series I

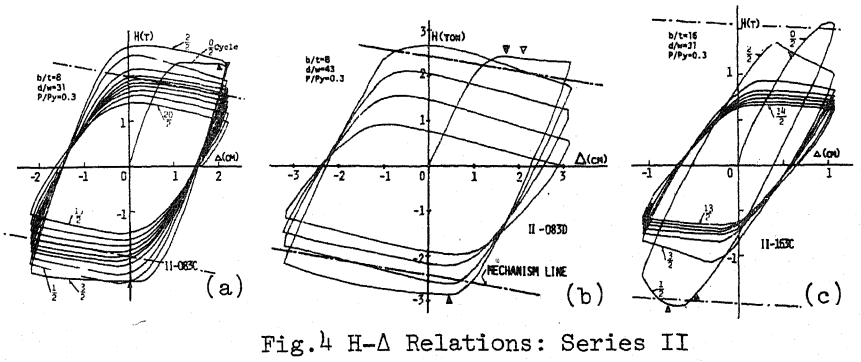

Fig.4 H-Δ Relations: Series II

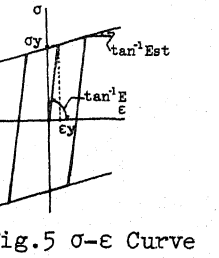

Fig.5 σ-ε Curve

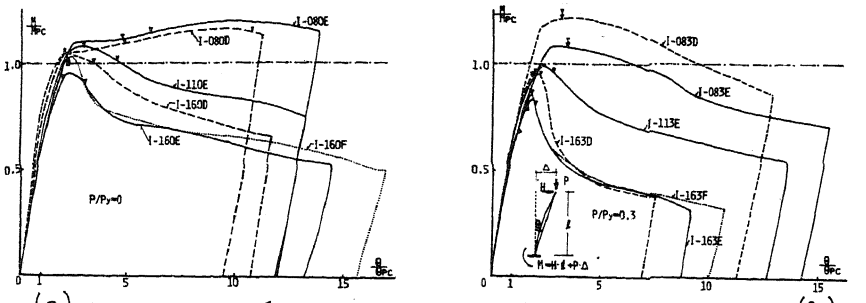

(a) (b)

Fig.6 Dimensionless M-θ Relations

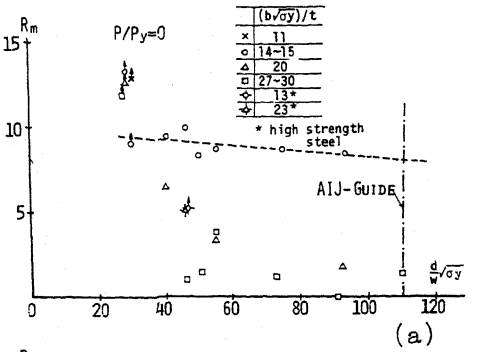

(a)

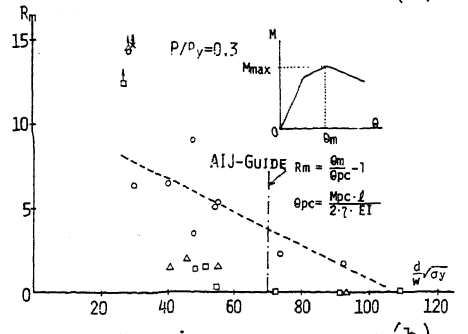

(b)

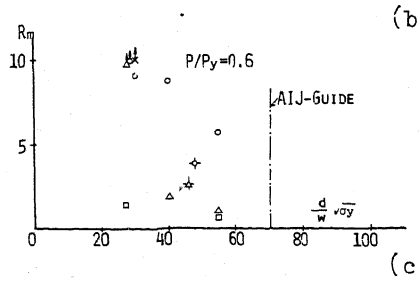

(c)

Fig.7 Plastic Rotation Capacity

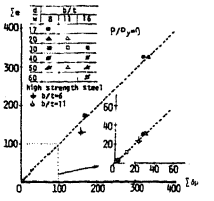

(a)

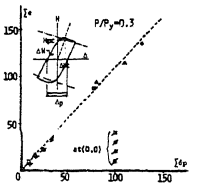

(b)

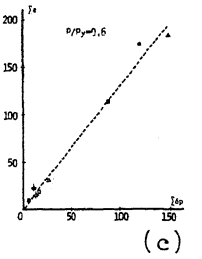

(c)

Fig.8 Σe-Σδp Relations

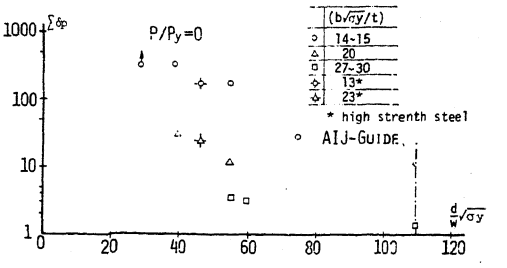

(a)

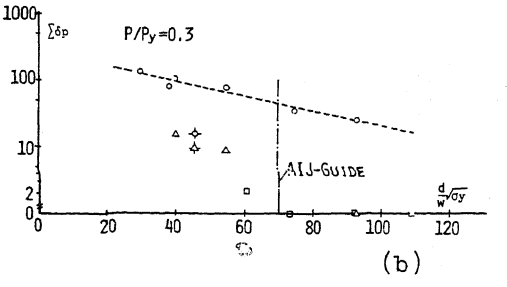

(b)

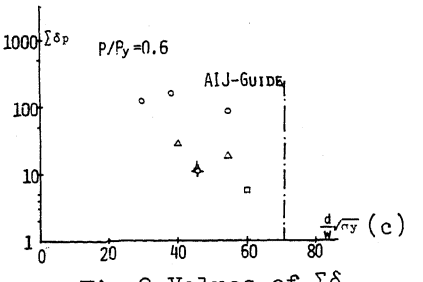

(c)

Fig.9 Values of $\Sigma\delta_p$

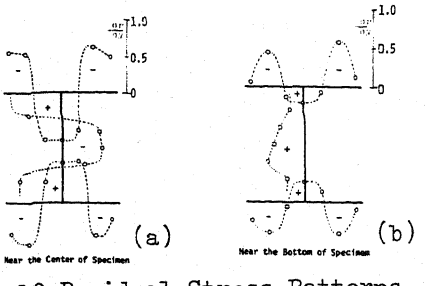

(a) (b)

Fig.10 Residual Stress Patterns

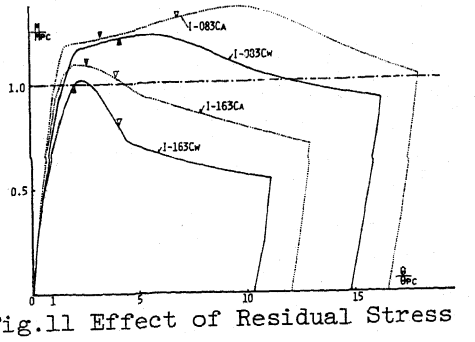

Fig.11 Effect of Residual Stress